Integrated array of 2-μm antimonide-based single-photon counting devices

M. A. Diagne,[1,2,*] M. Greszik,[1] E. K. Duerr,[1] J. J. Zayhowski,[1] M. J. Manfra,[1] R. J. Bailey,[1] J. P. Donnelly,[1] and G. W. Turner[1]

[1]*Lincoln Laboratory, Massachusetts Institute of Technology, 244 Wood Street, Lexington, Massachusetts 02420-9108, USA*
[2]*Dept of Physics, Connecticut College, 270 Mohegan Ave, New London, Connecticut 06320, USA*
**mdiagne@ll.mit.edu*

Abstract: A 32x32 Sb-based Geiger-mode (GM) avalanche photodiode array, operating at 2 μm with three-dimensional imaging capability, is presented. The array is interfaced with a ROIC (readout integrated circuit) in which each pixel can detect a photon and record the arrival time. The hybridized unit for the 1000-element focal plane array, when operated at 77K with 1 V overbias range, shows an average dark count rate of 1.5 kHz. Three-dimensional range images of objects were acquired.

OCIS codes: (100.2550) Focal-plane-array image processors; (250.1345) Avalanche photodiodes (APDs).

References and Links

1. E. K. Duerr, M. J. Manfra, M. A. Diagne, R. J. Bailey, J. P. Donnelly, M. K. Connors, and G. W. Turner, "Geiger-mode avalanche photodiodes at 2μm wavelength," Appl. Phys. Lett. **91**(23), 231115 (2007).
2. B. F. Aull, A. H. Loomis, D. J. Young, R. M. Heinrichs, B. J. Felton, P. J. Daniels, and D. J. Landers, "Geiger-mode avalanche photodiodes for three-dimensional imaging," Lincoln Lab. J. **13**, 335–350 (2002).
3. D. Boroson, A. Biswas, and B. Edwards, "MLCD: Overview of NASA's mars laser communications demonstration system," *Proceedings of SPIE - Free-Space Laser Communication Technologies XVI* **5338**, 16–28 (Jun 2004).
4. I. Andreev, M. Afrailov, A. Baranov, M. Mirsagatov, M. Mikhailova, and Y. Yakovlev, " Avalanche multiplication in photodiodes structures using GaInAsSb solid solutions," Sov. Tech. Phys. Lett. **13**, 199–201 (1987).
5. K. E. Jensen, P. I. Hopman, E. K. Duerr, E. A. Dauler, J. P. Donnelly, S. H. Groves, L. J. Mahoney, K. A. McIntosh, K. M. Molvar, A. Napoleone, D. C. Oakley, S. Verghese, C. J. Vineis, and R. D. Younger, "After pulsing in Geiger-mode avalanche photodiodes for 1.06 μm wavelength," Appl. Phys. Lett. **88**, 133503 (2006).
6. J. P. Donnelly, E. K. Duerr, K. A. McIntosh, E. A. Dauler, D. C. Oakley, S. H. Groves, C. J. Vineis, L. J. Mahoney, K. M. Molvar, P. I. Hopman, K. E. Jensen, G. M. Smith, S. Verghese, and D. C. Shaver, "Design considerations for 1.06-μm InGaAsP-InP Geiger-mode avalanche photodiodes," IEEE J. Quantum Electron. **42**(8), 797–809 (2006).
7. J. J. Zayhowski, and A. L. Wilson, Jr., "Energy-scavenging amplifiers for miniature solid-state lasers," Opt. Lett. **29**(11), 1218–1220 (2004).
8. J. J. Zayhowski, and C. Dill III, "Diode-pumped passively Q-switched picosecond microchip lasers," Opt. Lett. **19**(18), 1427–1429 (1994).
9. J. J. Zayhowski, "Periodically poled lithium niobate optical parametric amplifiers pumped by high-power passively Q-switched microchip lasers," Opt. Lett. **22**(3), 169–171 (1997).

1. Introduction

Individual antimonide-based Geiger-Mode (GM) avalanche photodiodes operating at 2-μm wavelength have previously been reported [1]. In this work, we present an extension of the earlier work to demonstrate a GM focal plane array operating at 2 μm. A focal plane array consisting of such photon-counting APDs is highly desirable for many applications ranging from 3-D laser radar [2] to photon-counting optical communications [3]. To demonstrate imaging at 2 μm with GM APDs, a 32x32 array was fabricated and then hybridized to a readout integrated circuit (ROIC) via indium bump bonding. The ROIC is a timing circuit that operates in framed (ladar) mode as described schematically in Fig. 5. The photon-timing

#138144 - $15.00 USD Received 15 Nov 2010; revised 27 Dec 2010; accepted 29 Dec 2010; published 17 Feb 2011

aspect of the ROIC is discussed later in this paper. In Geiger-mode operation, every APD, which is bump-bonded (or hybridized) to a node on the CMOS circuit, is biased above its breakdown voltage for a fixed duration at a regular interval. If a photo-generated carrier (or defect-related carrier in the dark) enters the high field region during this gate, the APD begins breaking down [4]. Finite capacitance on the circuit node, as well as series resistance in the circuit and internal space-charge effects limit the total current at breakdown. This current flow through the APD discharges the finite capacitance on the circuit node. The discharge directly triggers the CMOS digital logic in the ROIC. The GM APD/ROIC unit works as a photon-to-digital converter which produces a digital-logic-compatible voltage transition in response to a single photon. This approach provides a significant advantage in an array format as compared to linear mode APDs and photomultiplier tubes that come with more power dissipation related to the requirements of low-noise linear amplification. Dark count rate (DCR) and photon detection efficiency (PDE) are two important parameters used to characterize the performance of Geiger-mode APDs. Dark counts are generated by thermally-generated or tunneling-generated carriers from either the absorber or multiplication region that initiate Geiger-mode breakdown. After a GM APD has broken down, it is likely to be followed by an additional dark count known as an afterpulse [5] if the APD is immediately re-armed for detection of another incident signal photon. To prevent this afterpulsing, a reset time is required to allow the APD to empty traps that are filled with carriers. PDE is the product of three probability processes: quantum efficiency (QE) in the absorber, electron-hole injection in the multiplication region, and the probability of avalanche, thus PDE = QE x P_{inj} x PA. In that sense, PDE can be seen as the probability that a photon be absorbed to create an electron-hole pair causing an avalanche in the multiplication region. For improved APD performance, it is essential to reduce the DCR without degrading PDE, and it is often challenging to maintain a low dark count rate, while increasing the overbias required for higher photon detection efficiency. Single 30-µm-diameter devices of the GM APD array show an injection probability-avalanche probability product of 35% and dark count rates of 210 kHz at 77 K, and we believe that this high DCR is due to afterpulsing.

2. **Device structure and array fabrication**

The 2-µm APD structure, a separate absorber-multiplier (SAM) design [6], is grown by molecular beam epitaxy and consists of a lattice-matched $In_{0.15}Ga_{0.85}As_{0.17}Sb_{0.83}$ absorber, an $Al_{0.55}Ga_{0.45}As_{0.05}Sb_{0.95}$ multiplication layer, and a thin field stop layer separating the absorber and the multiplier as shown in the schematic representation of an APD cross-section in Fig. 1.

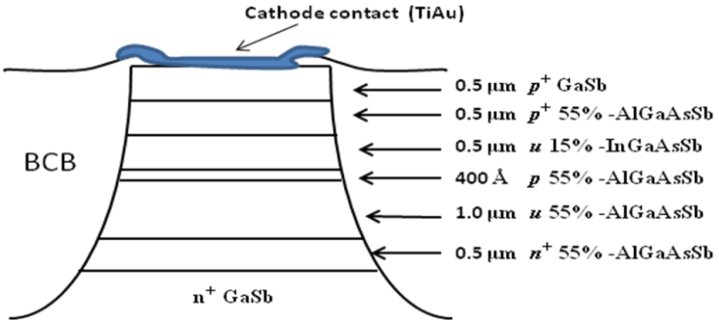

Fig. 1. Schematic of mesa isolated 2µm Sb-based SWIR APD.

The 32x32 mesas of the array, 30 µm in diameter on a 100–µm-pitch, are formed using conventional contact photolithography and etching 3.5 µm into the epitaxial layers (down to GaSb bottom contact layer) using a mixture of 1:10:67:300 HF:H_2O_2:H_2O:$C_6H_8O_7$. The wet etch mixture is very effective in removing the native oxide buildup prior to surface passivation and also provides damage free surfaces. Dry etching techniques have also been

#138144 - $15.00 USD Received 15 Nov 2010; revised 27 Dec 2010; accepted 29 Dec 2010; published 17 Feb 2011

explored but showed signs of significant sidewall damage and resultant increases in leakage current. Benzocyclobutene (BCB), a photosensitive polymer is chosen for surface passivation because of its thermal stability, low moisture content, low cure temperature and high degree of planarization. The BCB polymer is patterned to access contact areas prior to a 210°C cure in nitrogen atmosphere for 1 hour. A layer of Ti/Au (300Å/2000Å) is deposited for the contact to both the anode and cathode of the APD.

3. Focal plane arrays of SWIR APDs

Before integrating a GM-APD array with a ROIC, breakdown uniformity was measured on an electrical probe station at room temperature. Shown in Fig. 2 is a map of the breakdown voltage of the array showing less than 1 V of variation in breakdown voltage. Breakdown voltage uniformity is essential to allow efficient avalanche detection and the subsequent triggering of the timing circuit by each APD when the entire array is biased with a single voltage, as this is a limitation in the present ROIC design. Because of the high voltage applied to the common cathode contact, a single shorted APD can lead to catastrophic failure of the entire focal plane array. Therefore, the entire array is initially probed and leaky devices are electrically isolated prior to the hybridization in order to avoid a rapid rise in current caused by shorting the ROIC. When discrete APDs are testing in a probe station or wire-bonded package, the capacitance discharged through the APD during breakdown includes not only the APD capacitance but the parasitic capacitance of the wire bond or probe and the capacitances of the cabling and bias tee. These cable and bias tee capacitances can be quite large such that the voltage on the APD does not drop significantly until the pulse generator used to overbias the APD lowers the voltage below breakdown at the end of the measurement gate. In this configuration, the charge flow through the APD is typically in the range of 1 to 10 nC. By contrast, the APD hybridized to ROIC needs only discharge its own capacitance and the parasitic capacitance of the bump-bonded ROIC, typically 150 fF. Because the APD turns off soon after the overbias of 3.1 to 4.1 V is discharged, the total charge flow through the APD is less than 1 pC.

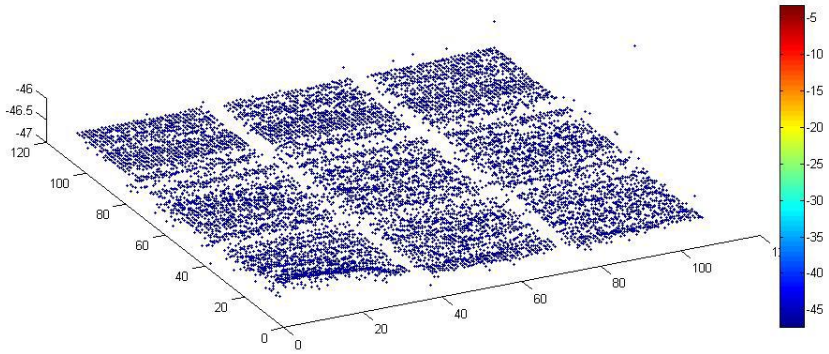

Fig. 2. Breakdown uniformity measured for a 2μm 32 x 32 array.

To establish electrical contact to the ROIC, 15 μm of indium is deposited on top of each mesa of the 32x32 array of avalanche photodiodes by lift-off process. The array is then bump bonded to the CMOS ROIC using an FC-150 Karl Suss hybridization system. The hybridized unit is then underfilled with Hysol, an epoxy with low viscosity and cured at 80°C on a hotplate for 3 hours. The underfill and curing process is needed to provide mechanical integrity for all subsequent handling, as well as for cryogenic operation. With the exception of the substrate, the hybridized unit is masked with photoresist and the substrate polished in bromine-methanol to reduce the backside substrate roughness and optical scattering losses. The assembled detector/readout is then cleaned, epoxied and wire-bonded to a ceramic

#138144 - $15.00 USD Received 15 Nov 2010; revised 27 Dec 2010; accepted 29 Dec 2010; published 17 Feb 2011

submount leadless chip carrier, as shown in Fig. 3. The ceramic submount was then clamped to the cold finger of a Stirling-cycle cooler in a Dewar to enable cooling the focal plane array, as shown in Fig. 4. All control and data output electrical signals were routed outside the Dewar via high-thermal-resistance lines. The overall cooler assembly weighs 5 kg and requires a relatively low power (24-V, 1-A) dc power supply.

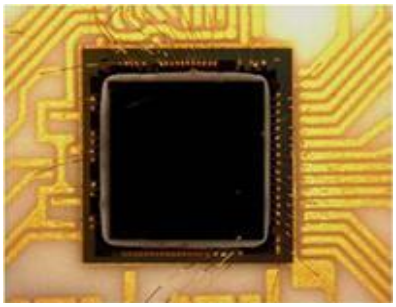

Fig. 3. Photograph of 2-μm APD array hybridized to CMOS ceramic IC and wire bonded to submount.

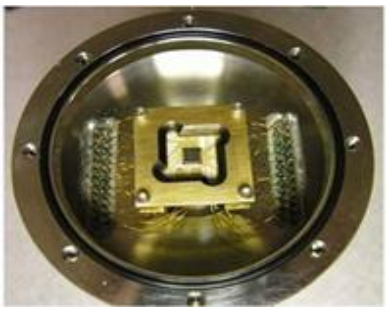

Fig. 4. Photograph of focal plane array on submount in Dewar.

The ROIC used in this experiment is configured to work in framed mode as would be utilized in a ladar system. A range gate clock is started behind each pixel, and for each APD breakdown event detected, the circuit behind the pixel stops counting in order to time-stamp the photon's arrival (or the dark count). The counter in the pixel is counting clock cycles, and the arrival of the photon stops counting the cycles and locks that value as timing value with a 2-ns least significant bin width. At the end of the range gate, all time-stamps and locations are recorded. The ROIC does not record any new data during a 400-µs window, while transferring the data off chip. The 400-µs long dead time is due to a 2.5 kHz maximum pulse rate of the particular implementation of the laser. A schematic of the framed ROIC operation timeline is shown in Fig. 5.

#138144 - $15.00 USD Received 15 Nov 2010; revised 27 Dec 2010; accepted 29 Dec 2010; published 17 Feb 2011

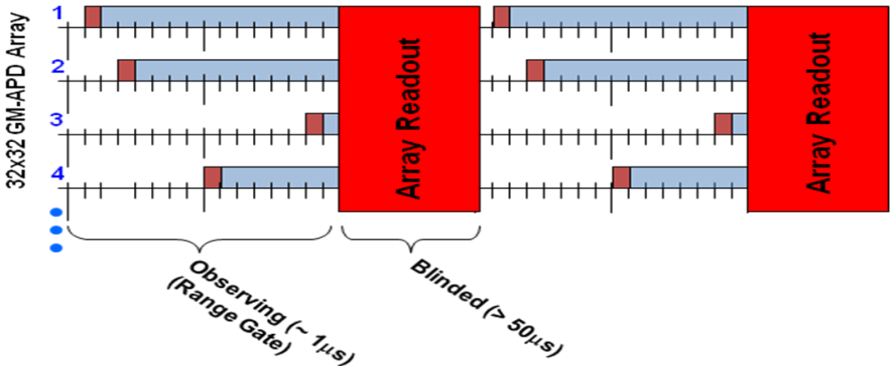

Fig. 5. Framed ROIC architecture.

4. Experiments and results

For laser radar measurements with the integrated GM APD array, a custom tunable microchip laser source was developed. The laser source is pumped by a passively Q-switched [7, 8] Nd:YAG (neodymium-doped yttrium-aluminum-garnet) laser which is itself pumped with a 808-nm cw diode pump laser. The 1.064-μm pulse produced from the microchip laser is used to pump a periodically poled lithium niobate (PPLN) [9] crystal patterned with a linear array of gratings. The high peak power of the pump generates difference wavelengths through optical parametric down conversion. Wavelengths ranging from 1.5- to 3.5-μm are achievable by selecting the appropriate grating and temperature of the PPLN. For each grating and temperature setting, a signal and idler photon are generated, and the desired wavelength is selected by external filtering. Pulses, 400-ps in duration, with at least 3-μJ of energy and up to 10-kHz repetition rate are produced. The broadband source parameters are displayed in Fig. 6.

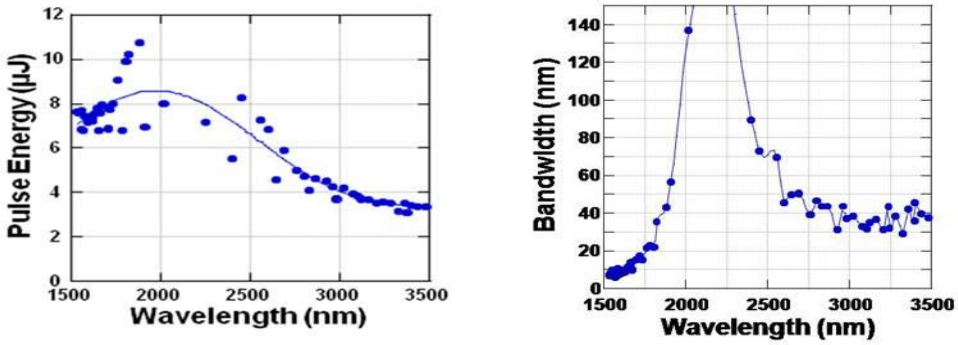

Fig. 6. Output pulse energy and bandwidth of the microchip laser source.

Dark count rates were recorded for all bias levels, and an average dark count rate (DCR) of the array elements was measured (Fig. 7a). The DCR measured in the hybridized array is lower than measured on individual GM APD devices, and we believe the difference is due to an afterpulsing component in the individual device measurements. The array elements are less susceptible to afterpulsing because of the lower capacitance and smaller breakdown current flow through each element when hybridized on the ROIC. Relative photon detection efficiency (PDE) at several overbiases ranging from 3.1 to 4.1 V is also displayed in Fig. 7a. Measurements of PDE are made by shining the 2-μm beam on a diffuse target and plotting the relative response of the pixels imaging the spot. An intensity image is acquired by placing a human hand in front of the diffuse target illuminated by 2-μm pulses from the microchip laser (Fig. 7b). The pixel brightness in the image corresponds to the average firing rate of the pixel.

#138144 - $15.00 USD Received 15 Nov 2010; revised 27 Dec 2010; accepted 29 Dec 2010; published 17 Feb 2011

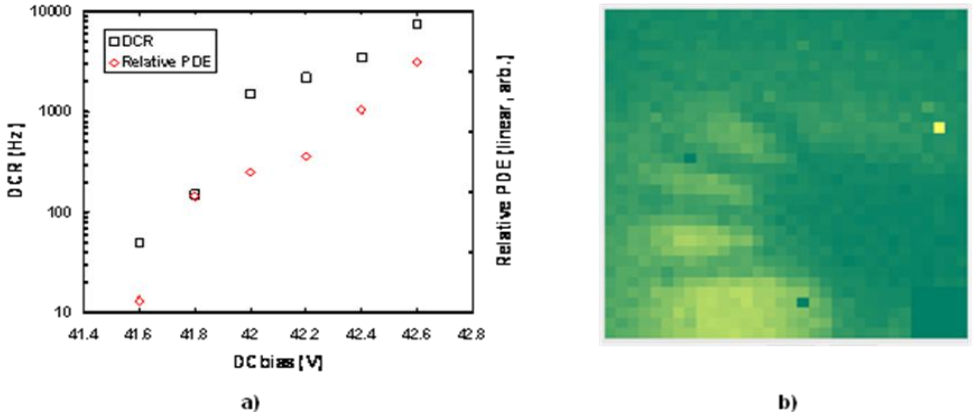

Fig. 7. (a) Average dark count rate and relative detection efficiency for 1000-element 2-μm Geiger-mode APD focal plane array. Overbias range: 3.1 – 4.1 V. (b) Intensity image of a human hand in front of a target illuminated with 2-μm radiation.

A demonstration of the three-dimensional imaging capabilities of this ladar system was performed by imaging the pyramid mounted on a tripod at a range of approximately 20 m, as shown in Fig. 8a. The range data corresponding to the pyramid and tripod in the photo is shown in Figs. 8b and 8c. The ROIC used in this work is primarily designed for n-on-p silicon or InP-based APDs instead of Sb-based p-on-n in this work which reversed the arm and disarmed functions on the chip. The non-optimum ROIC polarity issue is the origin of the relatively large range steps, due to the fact that the two least significant timing bits are not captured. Thus the minimum time step is 2 ns, which corresponds to approximately 30 cm (1 ft) in range because the time of flight measured is roundtrip time.

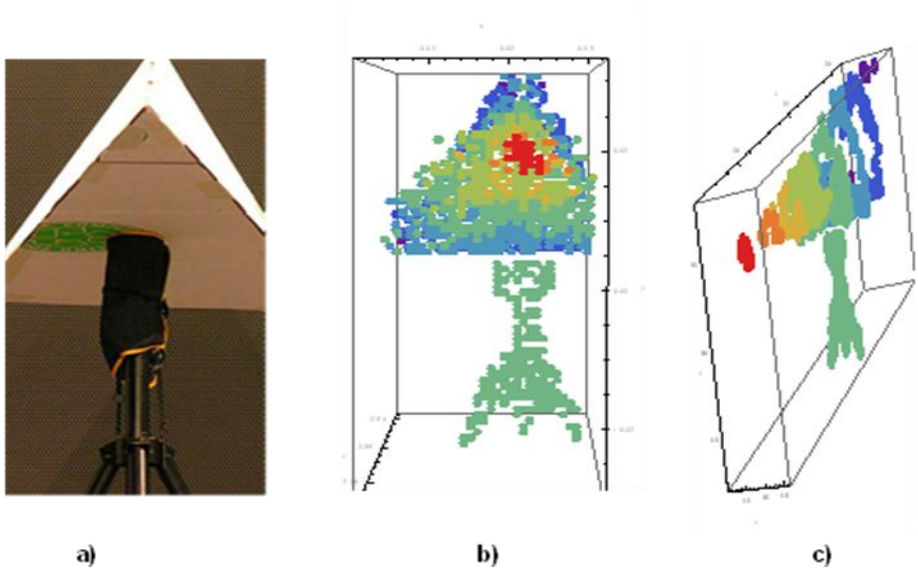

Fig. 8. (a) Pyramid on tripod, (b) 3D image of pyramid on tripod, c) Angle view of 3D ladar data of pyramid and tripod taken at 2-µm.

5. Conclusion

We have demonstrated the development of 2-µm 32 x 32 GM APD focal plane arrays with three-dimensional imaging capabilities, using the GaSb-based material system. These

#138144 - $15.00 USD Received 15 Nov 2010; revised 27 Dec 2010; accepted 29 Dec 2010; published 17 Feb 2011

hybridized arrays have shown an average dark count rate of 1.5 kHz at with an overbias ranging from 3.1 to 4.1 V, when operated at 77K. To enable ladar measurements, a compact broadly-tunable pulsed source was also developed by cw pumping of a passively Q-switched Nd:YAG laser. The laser produced at least 2 μJ pulses, 400-ps width and up to a 10-kHz repetition rate. Three-dimensional range imaging, with a 30-cm resolution at 20-m, was achieved with the combination of the 2-μm 32 x 32 GM APD array and custom laser.

Acknowledgments

This work was sponsored by the Defense Advanced Research Projects Agency (DARPA) under Air Force Contract No. FA8721-05-C-002. The opinions, interpretations, conclusions, and recommendations are those of the authors and are not necessarily endorsed by the United States Government.

#138144 - $15.00 USD Received 15 Nov 2010; revised 27 Dec 2010; accepted 29 Dec 2010; published 17 Feb 2011